Paper ID ILASS08-2-6

ILASS 2008
Sep. 8-10,2008, Como Lake, Italy

LINKING NOZZLE FLOW AND PRIMARY BREAKUP OF HIGH PRESSURE DIESEL JETS USING CFD

Oscar J. Soriano*, Rossella Rotondi

Diesel Systems, Hydraulic Simulation, Continental Automotive GmbH, Regensburg, Germany

ABSTRACT

In this paper, two models for the primary breakup of Diesel jets are analysed and compared, not only by means of simulations, but also to experimental data. Both models are based on the estimation of the potential breakup capability of the nozzle flow in order to obtain the size and velocity of the first droplets created out of the liquid jet. The used geometries for this investigation are real size nozzles like the ones encountered in passenger cars nowadays, operated under engine-like conditions. Unsteady simulations of the turbulent and multiphase flow inside the nozzle are carried out with the commercial 3D-CFD code CFX and are used as input for the spray simulations. Using this nozzle flow information, the primary break-up models of Tatschl [20] and Baumgarten [3] are applied to a standard injection case and their performance is evaluated. In the first case, the model is implemented in the 3D-CFD code FIRE, whereas CFX is used in the latter case.

INTRODUCTION

Achieving better atomization of the fuel spray to enhance heat and mass transfer in the combustion chamber is the most important issue in order to decrease emissions and meet future emission legislation standards. For Diesel engines, pollution formation is strongly influenced by the condition of the mixture during combustion, and the state of the mixture depends on the evolution of the fuel spray. Using a powerful tool like CFD simulation on the development process might be of a great help in investigating atomization and improving the proper spatial and temporal distribution of the mixture.

The fundamental mechanisms of atomization have been under extensive experimental and theoretical study for many years [13, 7, 6]. Today it is accepted, that the breakup of liquid jets under high-pressure injection conditions can be divided in two sub-processes: primary and secondary breakup [3, 16]. In the case of primary breakup it is assumed that the main mechanisms that lead to the first breakup of the coherent liquid column into big liquid drops and ligaments can be found inside the injection nozzle. The most cited mechanisms found in the literature are cavitation and turbulence [5, 3, 6, 22]. These are caused by the big pressure differences (about 2000 bar) and the tiny geometrical dimensions of the nozzle ($D = 150\mu m$), which lead to very high velocities and low static pressures, locally under saturation pressure of Diesel. The further breakup of the big drops and ligaments due to the aerodynamical interaction with the surrounding gas outside the nozzle is known as secondary breakup.

While many models dealing with the secondary breakup can be found in the open literature (listed in [3], very few have been developed to account for the important effects of the nozzle flow on the first disintegration of the coherent liquid column leaving the nozzle. In the last few years a great effort is being made trying to describe the primary breakup, not without considerable difficulties, mostly because of the lack of experimental studies focusing on this issue [2, 10, 3, 21].

For the mathematical description of the spray two approaches are used: the homogeneous (Euler/Euler) and the inhomogeneous (Euler/Lagrange) approach. Contrary to the homogeneous approach the inhomogeneous approach allows mass, momentum and energy exchange between the droplets and the gas phase, which is indispensable for Diesel spray calculations. Due to the easier implementation of the physical models and the robustness of the mathematical approach, a stochastic Lagrangian description of the Diesel spray is widely used in the literature, both for the secondary and primary breakup. According to this methodology, all processes, which cannot be resolved deterministic on a parcel level, are solved with a Monte-Carlo-simulation. This approach is in the case of secondary breakup extensively accepted, whereas for the primary some authors consider the homogeneous approach to be more efficient [22]. For this work, the Lagrangian approach will be used both for the primary and secondary breakup.

Due to this simulation approach the spray calculation starts with already existing drops that are subject to the interaction with the surrounding gas. The properties of these drops such as velocity direction (spray angle) and size distribution are an output of the primary breakup of the jet, which in most of the CFD-codes is usually not modeled but replaced with assumptions or even with experimental input. Today it is well known that this method of treating the primary break-up is not sufficient at all.

For this reason, several new models for cavitation and turbulence induced primary break-up have been developed in the last years, aiming to link the flow inside the nozzle with the spray atomization in a proper way. Different turbulent and cavitating conditions inside the injection holes result then in different spray structures and cone angles near the nozzle exit.

SPECIFIC OBJECTIVES AND SIMULATION APPROACH

Primary breakup models for Diesel injection applications differ in the way of handling the influence of cavitation and tur-

*Corresponding Author

bulence of the nozzle flow on the spray atomization. The main objective of this investigation is to compare the performance of two of the most widely used primary breakup models found in the literature accounting for cavitation and turbulence. The first model to be considered in this investigation is a modified version of the primary breakup model of Baumgarten [3], which was implemented in the commercial CFD-code CFX of Ansys [1]. The second one is the breakup model of Tatschl [20], available as a feature in the commercial CFD-code FIRE, of AVL-Technologies.

The simulation approach comprehend the unsteady simulation

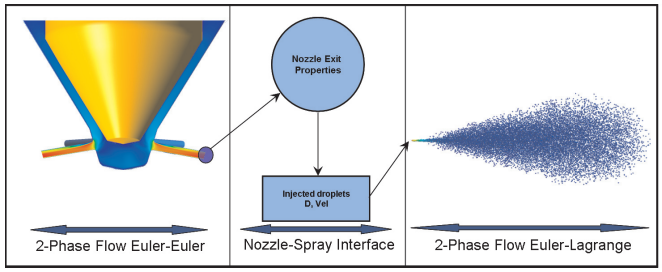

Figure 1: Simulation Approach

of the nozzle flow, recording the spatial distribution of the flow properties $(\vec{v}, \rho, k, \epsilon)$ at the nozzle exit as a function of time, both for Diesel fuel and Diesel vapour. These properties are then used as a boundary condition for the subsequent unsteady Lagrangian spray calculations, yielding initial conditions for the spray velocities, injected mass and available breakup energy. The unsteady simulation of the nozzle flow, including moving needle (injector opening) was also carried out with CFX.

The performance of both primary breakup models is also compared to optic spray measurements, including spray penetration $S_p(t)$ and near and far spray angles. All measurements were carried out in the test facilities of Continental Automotive GmbH in Regensburg, Germany.

NOZZLE FLOW SIMULATION

The spray breakup models use detailed information from 3D turbulent cavitating nozzle flow simulations performed with the Ansys CFX CFD code based on a Volume of Fluid (VOF) method [23]. This model was chosen because it offers a good compromise between computational effort and results quality. The VOF-model assumes that phases share the same pressure and velocity. The two-phase flow is considered homogeneous, isothermal and the liquid and vapour phases incompressible, having constant density values. The calculations are time-dependent because of the highly transient behaviour of the nozzle flow, specially in the needle opening phase.

The simplified Rayleigh-Plesset model is employed for the mass transfer term between phases. This model bases on the growth of a single spherical bubble in an unbounded liquid domain [4]. The SST shear stress transport turbulence model is employed in the simulations [1], assuming the flow to be fully turbulent.

Figure 2 shows the geometry of the studied nozzle. The geometrical parameters are listed in Table 1. Both holes have different values of included angle (IA), which is the angle included between the injector axis and the injection hole axis. Higher included angles show higher tendencies to cavitate and to produce

Inj. Hole	$HE(\mu m)$	$IA(^\circ)$	$CF(-)$
1	11	72	0.675
2	11	88	0.6

Table 1: Geometrical parameters of the studied nozzle

an asymmetric flow inside the hole. Here, CF (conicity factor) and HE (inlet rounding) are typical geometrical parameters of Diesel injection nozzles [9], where

$$CF = \frac{D_{in} - D_{out}}{L_{hole}} \cdot 100 \tag{1}$$

Low values of CF and HE cause high curvature of the streamlines, promoting cavitation.

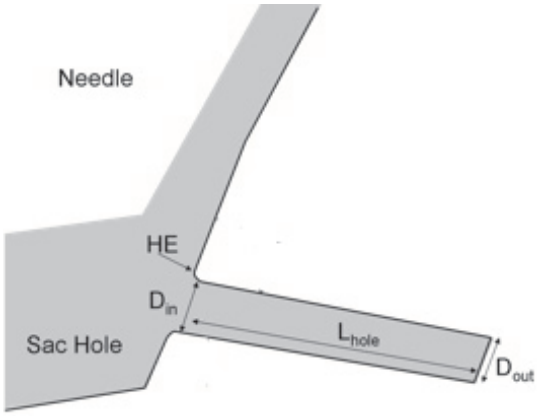

Figure 2: Scheme of nozze tip. Geometrical parameters

PRIMARY BREAKUP MODELS

Modified Baumgarten Model

In this model, the acting atomization mechanisms (turbulence and cavitation) are assumed to be present in the liquid jet as break-up energy. Basing on the spatial and temporal distribution of this break-up energy at the nozzle exit, properties of the injected droplets like size D and velocity $\vec{v}$ are calculated.

The break-up energy is estimated by means of a two-phase flow simulation of the nozzle. After that, an energy balance is drawn in order to calculate the properties of the injected droplets. These droplets are then introduced into a rectangular mesh of hexagonal cells, which will be shown later. The probability for new particles to be created at a certain position of the nozzle exit depends on the spatial resolution of the mass flow at the nozzle exit, so that a higher mass flow is represented by a higher number of particles. The spray angle is given by the diverging velocities described in the initial droplet velocity vectors $\vec{v}$. With this coupled approach, no initial value from empiric correlations needs to be used in the simulation chain and asymmetries in the nozzle flow are reproduced in the spray.

This coupling method is convenient when dealing with the atomization of non-axial symmetric liquid jets penetrating in dense gaseous ambient with very high velocities like the ones encountered in high pressure Diesel injection. Under these conditions a very fast disintegration of the coherent liquid flowing in the nozzle into drops of different sizes and shapes is expected.

This assumption of a very short intact core length can be found quite often in the literature [16]. Thus, the present numerical transition of the Eulerian two-phase flow in the nozzle into the Lagrangian two-phase particle flow in the chamber should offer a good approach to the problem.
The break-up energy consists of the two following terms: flow-induced turbulent kinetic energy [3, 2] and cavitation induced turbulent kinetic energy [21, 3, 10]. Turbulent fluctuations acting on the surface of a jet cause instabilities which lead to break-up. The same approach is used when considering the instabilities caused when modeling the released energy of collapsing cavitation bubbles: only the induced instabilities near the surface are assumed to contribute to the break-up. Flow induced turbulent kinetic energy is a direct output of nozzle flow simulation, while cavitation induced turbulent kinetic energy has to be calculated by resolving the cavitation bubble dynamics [3].
As a first step, the flow at the nozzle exit is divided in two zones depending on the liquid and gas contents. Cells with a volume fraction of vapour $VF > 0.1$ belong to the cavitating zone (zone 2) and the rest to the liquid zone (zone 1), as seen in figure 3. Then, a cylindrical control volume for the energy balance is defined, where the length is equal to the effective diameter of the liquid zone. After that, the break-up energy is evaluated for each zone as follows:

$$E_i = \eta_i \cdot (E_{cav,i} + E_{kin,turb,i}) \tag{2}$$

Here, i=zone 1 or zone 2 and η represent the efficiency of the energy transformation, and has a value of 1 for this first evaluation of the model.
It is assumed that the total break-up energy in zone 2 turns into

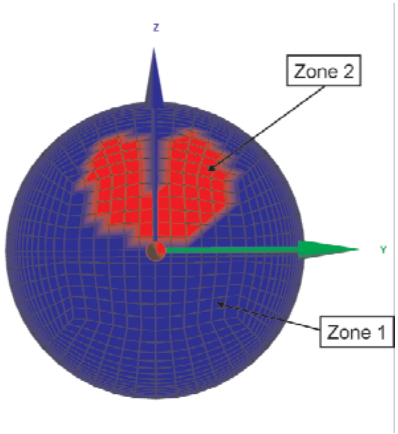

Figure 3: Typical distribution of zones at the nozzle exit

surface energy for the formation of the droplets and for their radial kinetic energy.

$$E_{2,eff} = E_{\sigma 2} + E_{kin2} \tag{3}$$

$$E_{\sigma 2} = \sigma \cdot \pi d_{cav}^2 \cdot n_2 \tag{4}$$

$$E_{kin2} = \frac{1}{2} \cdot v_{r2}^2 \cdot m_{droplet} \cdot n_2 \tag{5}$$

$$n_2 = \frac{6 \cdot m_2}{\pi \cdot d_{cav}^3 \cdot \rho_l} \tag{6}$$

For the liquid zone it is assumed that the total energy is present as turbulent fluctuations that act against the stabilizing surface forces [3]. Mass is split off the liquid zone until both forces are in equilibrium:

$$U_{turb} = \sqrt{\frac{2 \cdot E_1}{3 \cdot m_1}} \tag{7}$$

$$F_{turb} = \frac{1}{2} \rho_L \cdot u_{turb}^2 \cdot S \tag{8}$$

$$F_\sigma = 2 \cdot \sigma \cdot (2 \cdot d_{eff}) \tag{9}$$

$$C \cdot F_{turb} = F_\sigma \tag{10}$$

Here, S is the surface of the liquid where the turbulent disrupting force is acting. In order to obtain plausible values for the diameter of the injected droplets, it is necessary to multiply the disrupting force by a coefficient $C = O(10^{-2})$ [2].
The remaining mass is transformed to a cylindrical droplet and its energy content is used to calculate its radial velocity. The split mass undergoes then the same calculation of eq 5 to eq 7.

FIRE Model

This model takes into account the effects of turbulence, cavitation and aerodynamic interaction with air on the primary atomization of a liquid fuel jet. A competition between turbulence-cavitation and aerodynamic forces is implemented. Two timescales are evaluated and the smaller produces the atomization event with detached droplets having size related to the characteristic length scale.
The turbulence-cavitation induced atomization is accounted for by solving an equation for turbulent kinetic energy and its dissipation rate within the liquid fuel core. The collapse of cavitation bubbles enhances atomization through a source term, S_k, in the turbulence equation. The equations read as follows:

$$\frac{dk}{dt} = -\varepsilon + S_k \tag{11}$$

$$\frac{d\varepsilon}{dt} = -C_2 \cdot \frac{\varepsilon}{k} \cdot (\varepsilon - S_k) \tag{12}$$

Where C_2 is a model constant and the source term for cavitation, S_k, related to the change of the kinetic energy of the liquid around the bubble, is evaluated through the Rayleigh-Plesset equation [20]. The boundary conditions required, local fuel velocity, turbulence intensity and fuel vapor mass fraction, are provided by the nozzle flow simulations.
Equations 11 and 12 allow the evaluation of the relevant time and length scales:

$$\tau_t = C_\mu \frac{k}{\varepsilon} \tag{13}$$

$$r_t = C_\mu^{0.75} \frac{k^{1.5}}{\varepsilon} \tag{14}$$

where C_μ is given by the standard $k - \varepsilon$ model. The ligaments release positions are chosen randomly within the orifice cross section at each time step.
The aerodynamic induced primary atomization is the result of aerodynamic interaction between the liquid and the gas that induces unstable wave growth on the liquid jet surface. For this purpose the WAVE model [12] is used which is based on a first-order linear theory of stability analysis for liquid jets.
Curve fits of numerical solutions to the dispersion equations [14] provide the following expressions for the maximum growth rate Ω and the corresponding wavelength Λ:

$$\frac{\Lambda}{a} = 9.02 \frac{\left(1 + 0.45 Z^{0.5}\right)\left(1 + 0.4 T^{0.7}\right)}{\left(1 + 0.87 We_2^{1.67}\right)^{0.6}} \tag{15}$$

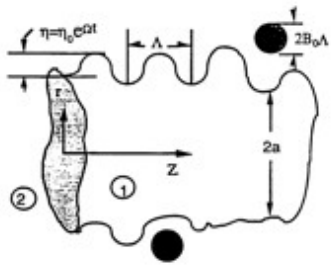

Figure 4: Schematic diagram showing surface waves and stripping on a liquid jet or blob of initial size a [12]

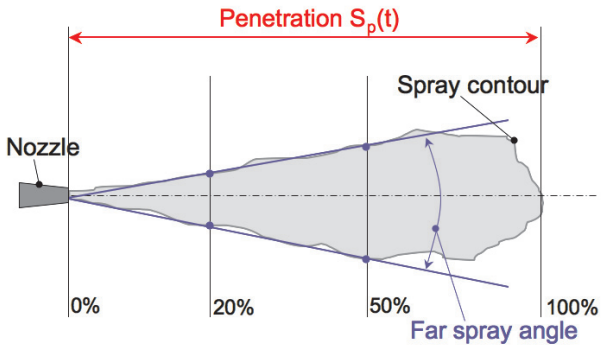

Figure 5: Definition of spray parameter

$$\Omega \cdot \left(\frac{\rho_L a^3}{\sigma}\right)^{0.5} = \frac{0.34 + 0.38We_2^{1.5}}{(1+Z)\,(1+1.4T^{0.6})} \tag{16}$$

where

$$Z = \frac{We_1^{0.5}}{Re_1} \qquad T = ZWe_2^{0.5} \qquad We_1 = \frac{\rho_L U^2 a}{\sigma}$$
$$Re_1 = \frac{Ua}{\upsilon_1} \qquad We_2 = \frac{\rho_G U^2 a}{\sigma} \tag{17}$$

The characteristic timescale τ is given by:

$$\tau = 3.726 B_1 a/\Lambda\Omega \tag{18}$$

After the atomization new droplets are stripped off the parent primary blob (see Fig. 4) with size r computed from the wavelength of unstable waves:

$$r = B_0\Lambda \quad \text{if } B_0\Lambda \leq a \tag{19}$$

and

$$r = min \begin{cases} (3\pi a^2 U/2\Omega)^{0.33} \\ (3a^2\Lambda/4)^{(0.33)} \end{cases} \quad \text{if } B_0\Lambda > a \tag{20}$$

The radius of the primary blob decreases according to:

$$\frac{da}{dt} = \frac{-(a-r)}{\tau} \qquad (r \leq a) \tag{21}$$

$B_0 = 0.61$ is the model size constant and B_1 is the model time constant depending on the injector characteristics and is assumed to be related to initial disturbance levels originating within the injector nozzle.

MEASUREMENTS

The spray visualization was performed using a high speed CCD camera [9]. Spray penetration and both near and far spray angles were obtained as a function of time for the investigated spray. The definition of the far spray angle and penetration can be obtained from Figure 5, where the mass of the spray is divided into three zones with 20%, 50% and 99% of the spray penetration. The near spray angle is defined as the angle between the spray contour for 20% of the spray penetration and the point of intersection between the injection hole axis and the injector axis.
The boundary conditions of the measurements and corresponding simulations can be found in Table 2. The injected liquid is ISO4113, which shows very similar properties as Diesel fuel. For the varying ambient conditions Nitrogen as ideal gas was used. At injection start, laminar flow is assumed in the injection chamber, with ambient temperature of about 25°C. This implies cold injection, with a very low vaporization rate.

Op. Point	$p_{inj}(bar)$	$p_{ch}(bar)$	$T(K)$	Gas_{ch}
1	800	20	298	N_2
2	1300	20	298	N_2
3	1600	10	298	N_2
4	1600	20	298	N_2
5	1600	40	298	N_2

Table 2: Operating points considered for the measurements.

SPRAY SIMULATION SETUP

Since the calculations are going to be performed with two different codes, care should be taken in choosing the same numerical setup. This condition is a little bit restrictive because both codes don't offer the same possibilities in order to model sprays. For example, collision and coalescence between droplets can't be considered for this investigation because both codes don't offer the same model to approach the problem and it would be a source of uncertainty for the comparison. Regarding the secondary breakup, the model of Reitz and Diwakar [15] was used because it was the only model present in both codes which offered plausible results for Diesel injection applications, even if other secondary breakup models like WAVE or CAB could offer better results. With this choice a worse agreement with experimental results is expected, but the comparison between spray simulations is more reliable.
For the description of the spray penetrating the dense gas ambient two phases are considered: the dispersed phase (fluid droplets) and the gas phase (continuum). The gas phase is modeled with the Eulerian approach using the Navier Stokes equations, while the dispersed phase is tracked through the flow in a Lagrangian way. The tracking is carried out by forming a set of ordinary differential equations in time for each particle, consisting of equations for position and velocity. The particle source terms are generated for each particle as they are tracked through the flow. Particle sources are applied in the control volume that the particle is in during the time step [17].
The concentration of the droplets in the fluid stream is high so that a two-way coupling is considered between the phases. This implies that the fluid affects the particle motion through the viscous drag and a difference in velocity between the parti-

cle and fluid, and conversely, there is a counteracting influence of the particle on the fluid flow due to the viscous drag. In addition to the drag forces (Schiller-Naumann), turbulent dispersion is also taken into account for these simulations. Although the gas-phase turbulence induced by this high-pressure-driven spray is anisotropic [11], an isotropic dispersion approach with the $k-\epsilon$ model is used. The initial turbulence levels are very low ($k = 1e^{-}4$ and $\mu_{turb} = 0.1$).
It is well known that the mesh can play an important role when simulating sprays with the Lagrangian approach. For this work an adaptive mesh was used (Fig. 6), so that for the perpendicular directions, the used lengths of a computational cell for the calculations are about 0.15 mm in the dense spray zone and 0.8 mm for far field of the spray. In the axial direction, an almost constant cell length of 0.8 mm was used. The domain has a total length of 10 cm in the axial direction and 2 cm in the other two perpendicular directions, which results in a total number of cells of about 10^5. For all calculations a parcel injection rate of $2 \cdot 10^8$ parcels per second was taken, which should be enough to deliver statistical convergence for the calculation.

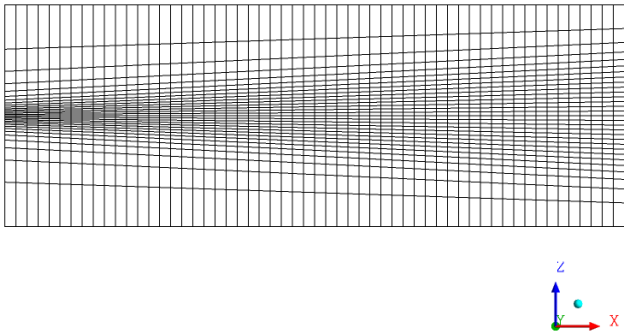

Figure 6: Mesh

RESULTS

Evaluation of the influence of the CFD Code and secondary breakup model

Since the spray calculations which are going to be compared in this paper are carried out with two different codes, an evaluation of the influence of the code seems meaningful before the performance of the primary breakup models is investigated. Even if both codes use the same Lagrangian approach for the calculation of sprays, there can always be some differences in the implementation which can affect the quality of the comparison.
In order to quantify the influence of the code, a simple spray calculation without primary and secondary breakup will be carried out for both codes CFX and FIRE. The boundary conditions of the simulations are representative for Diesel injection conditions. Droplets are injected with a size of $d = 100\mu m$ and a velocity of $U = 400m/s$. The injection angle is 20° and the pressure of the gas (N_2) 20 bar. Results regarding penetration are shown in figure 7. In the same diagram the results of the same calculation with secondary breakup activated are also shown in order to evaluate its influence on the results.
It can be seen that the results are very similar in the case the calculations without droplet breakup. That means that the drag force is evaluated in the same way by both codes. If the secondary breakup model of Reitz and Diwakar [15] is activated, results differ a little. There seems to be a little difference in the implementation of the secondary breakup model, which can affect the results and has to be taken into consideration.

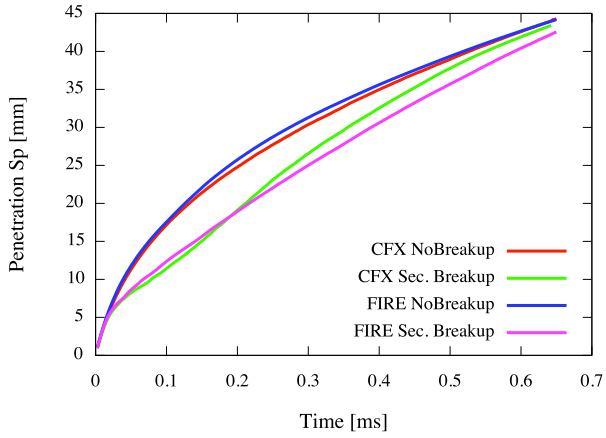

Figure 7: Penetration without droplet breakup and with secondary breakup for both investigated codes

Results of the spray simulation

Due to the limited length of this paper, all results shown in the following correspond to the injection hole 2 described in Table 1.
It can be seen in Figure 8 that the penetration for the FIRE model is higher and agrees better with the experimental values than the one calculated with the Baumgarten model. The reason for this can be found in the size of the primary droplets, which are bigger in the first case, as it will be shown later. Another reason for this behaviour is the axial position where primary droplets are created. In the case of this version[1] of the Baumgartens model implemented in CFX it is assumed that the primary breakup takes place right before the injection of the primary droplets [18]. That means, that the primary droplets to be injected into the domain have a certain size given by Eq. 10 and 4, smaller than the nozzle diameter. On the contrary, the calculations in FIRE inject droplets of the size of the nozzle

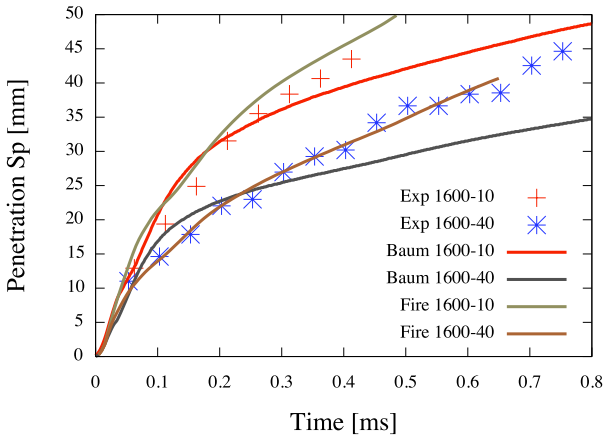

Figure 8: Experimental and numerical spray penetration for two different chamber pressures

[1] not in the original

diameter which then are object of the primary breakup. The primary droplets are then created after the original droplets have been tracked for a certain distance, which depends on the injection velocity and the corresponding timescale of Eq. 13 or 18. These both effects lead to a higher penetration of the spray. The results of the FIRE model agree quite well with the experimental data even if no interaction between droplets is taken into account, which is expected to have an influence.
The evaluation of both near and far spray angles shows that the investigated primary breakup models are able to predict an increase of the spray angle with the ambient density, following the trends found in the literature [16]. In Figures 9 and 10 the influence of the ambient pressure on both near and far spray angles for $t = 0.7ms$ is shown. The agreement with experimental results seems to be better for the Baumgarten model.
In Figure 11 a plot of the spray simulation in CFX and in FIRE

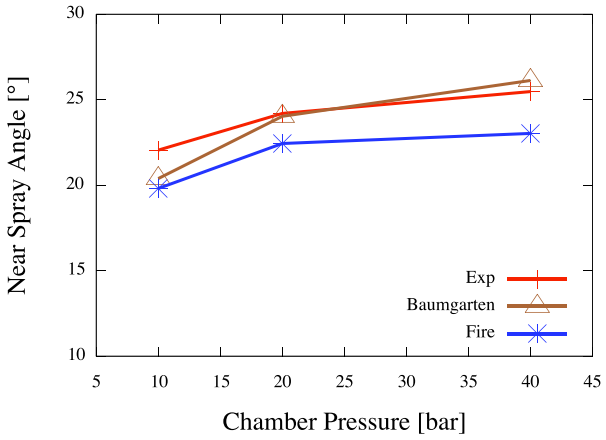

Figure 9: Experimental and numerical near spray angles for different chamber pressures at t=0.7 ms

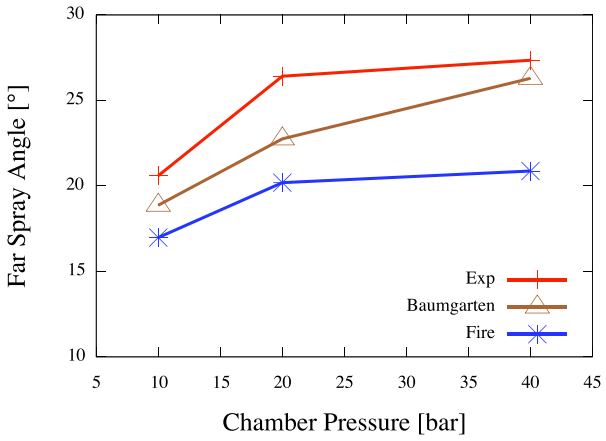

Figure 10: Experimental and numerical far spray angles for different chamber pressures at t=0.7 ms

is superposed to the picture of the spray for $t = 0.6$ ms and case 4 in Table 2, using the same length scale. For this time value, the agreement in the penetration is better for the simulation carried out with FIRE, but the overall contour and form of the spray seems to be better estimated by the calculations in CFX.

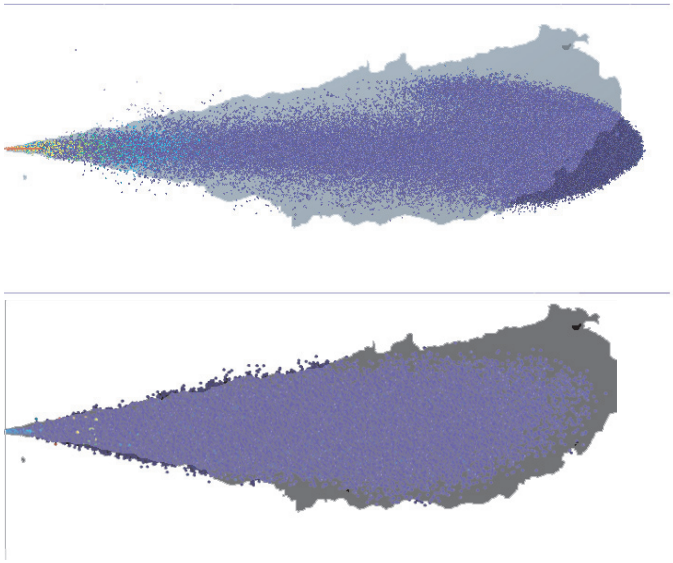

Figure 11: Experimental and numerical spray shape of inj. hole 2 at t=0.6 ms, (Top: FIRE; Bottom:CFX).

Performance of the primary breakup models

The depicted spray penetration and spray angles of Figures 8-10 show the results of the whole sprays computed by both codes, where the primary breakup model plays an important role. There are other issues though that can influence the computation, like the secondary breakup model. For the purposes of this paper, an evaluation of the output of the primary breakup model seems to offer a better basis in order to draw conclusions. An important variable for the evaluation of the performance of the models is the mean size of the injected primary droplets. Figure 12 shows the computed mean size for both codes together with the needle lift for the operating point 4 of Table 2. For the modified Baumgarten model, it can be seen that in the beginning of the injection the droplet sizes are of the order of magnitude of the nozzle exit diameter, because the flow in the injection hole is laminar and not cavitating. If the needle continues to open, the instabilities in the flow which promote increase and the primary droplets are smaller, indicating a better atomization.
There is a big difference on the computed values of the primary droplet size for the figure 12. Unfortunately it is not possible to evaluate the quality of the model out of the information on droplet sizes because there are no reliable experimental data in the literature. But it can be assumed that the predicted mean size of the FIRE model offers a better approach to the problem because the spray penetration shown in figure 8 agrees better with the experimental values. This also indicates that a lower value of the constant C in Eq. 10 is needed in order to get bigger droplets and therefore better penetration results for the model of Baumgarten.
Another important variable is the initial velocity of the primary droplets. Information about the mean axial velocity of the primary droplets is a direct output from the nozzle simulation and therefore is almost the same for both codes, since both computations use the same boundary conditions. The value calculated in both cases is approximately 540 m/s for fully opened needle conditions (operating point 4 in Table 2). On the contrary, the primary breakup models calculate different radial velocities (divergence), leading to different near cone angles (see Fig. 9). The near cone angle, and therefore the radial velocities, seem to

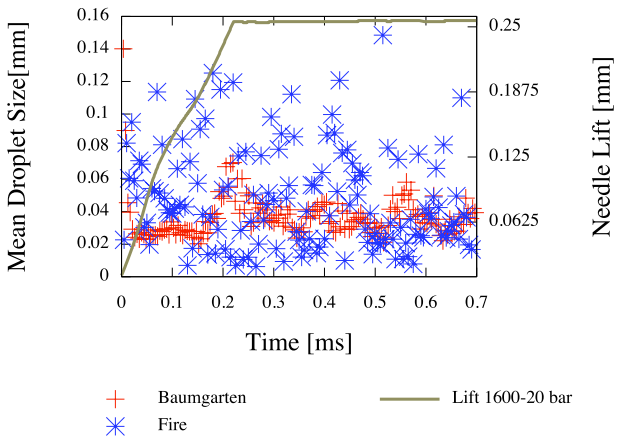

Figure 12: Mean primary droplet size and needle lift as a function of time

be better estimated by the Baumgarten model.
In the last years, some authors found out that not only the flow in the injection hole of standard Diesel injection nozzles is asymmetric [19, 18], but also the spray breakup [5, 8]. This has also been investigated in this paper for both codes. Results are depicted in Fig. 13, showing both the positive and negative half spray cone angle of plane XZ caused by the investigated primary breakup models, following the coordinates system shown in Fig. 6. Due to the cavitation appearance on the upper wall of the injection hole, the spray breakup calculated with the Baumgarten model shows a promoted primary breakup for positive values of Z-axis, causing a pronounced asymmetry of the spray. It can also be seen that the influence of cavitation is proportional to the ambient pressure following the Rayleigh-Plesset equation, so that the asymmetry is more pronounced for higher chamber pressures. The model in FIRE produces symmetric sprays and both half spray angles have the same values.

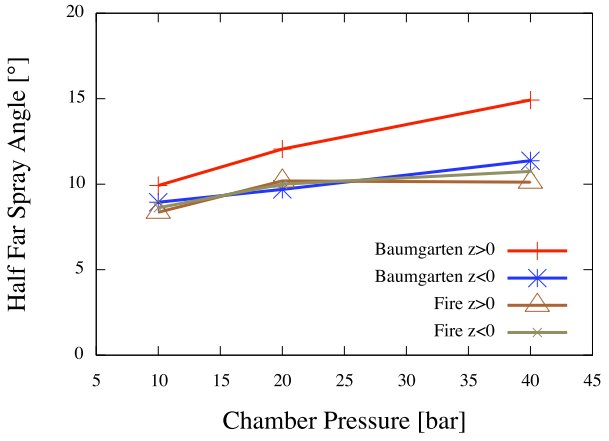

Figure 13: Numerical half far spray angles for different chamber pressures at t=0.7 ms

CONCLUSIONS

In this work a short performance study on Diesel spray breakup accounting for both primary and secondary spray breakup has been done. The aim was to find the most reliable tool in order to be able to reproduce the influence of the nozzle flow on the first disintegration of the liquid core flowing out of the injection nozzle. The analysis consists of the comparison of computations with optic spray measurements from a cavitating nozzle.
All results showed in this paper follow the tendencies found in numerous investigations of spray formation under Diesel injection conditions found in the literature. Both analysed primary breakup models are able to reproduce the general behaviour of Diesel jets in high pressure ambient conditions.
The better agreement of the penetration calculations with the Fire model indicates that the size of the primary droplets are more likely to be better estimated than in the model of Baumgarten. This implies that the constant C of Eq. 10 in the model of Baumgarten needs to be increased in order to get higher primary droplet sizes for future simulations.
Both primary breakup models yield similar values of near and far cone angles, showing an increase of the spray angle for high chamber pressures. Nevertheless the overall agreement regarding the spray shape seems to be better for the model of Baumgarten, which in addition to that offers the possibility of handling asymmetric sprays,
Form a general point of view, the primary breakup models investigated in this paper show a similar performance for high pressure Diesel injection conditions. A clear statement regarding the comparison between both models can not be easily made. In addition to that, a comparison between two models implemented in different codes has to be carefully carried out, for there is always a code dependency. A deeper validation accounting for spray velocity profiles in different axial positions and air entrainment seems to be the natural next step to discern which primary breakup model offers better performance under high pressure Diesel injection conditions.

NOMENCLATURE

Symbol	Quantity	Unit
CF	Conicity Factor	-
d	Droplet Diameters	m
D	Nozzle Diameters	m
E	Energy	$Kg \cdot m^2/s^2$
L	Length	m
HE	Inlet Rounding	m
IA	Included Angle	$^\circ$
$\dot{m}$	Mass flow	Kg/s^{-1}
n	Number of droplets	-
p	Pressure	bar
r	Droplet Radius	m
S_p	Penetration	m
t	Time	s
VF	Volume Fraction	-
Greek Letters		
η	Efficiency	-
ω	Surface Tension	N/m
Ω	Surface Growth Rate	s^{-1}
Λ	Wavelength	m
μ	Dynamic Viscosity	$Kg/m \cdot s$
τ	Timescale	s

Subscripts

1	Liquid Zone
2	Cavitation Zone
ber	Bernouilli
cav	Cavitation
eff	Effective
exp	Experiment
geg	After Nozzle
G	Gas
in	Inlet
inj	Injection
kin	Kinetic
L	Liquid
out	Outlet
r	Radial
rem	Remaining Mass
sim	Simulation
spl	Split Mass
turb	Turbulence
vor	Before Nozze

References

[1] *ANSYS CFX-Solver Theory Guide*. Ansys Europe, Ltd., 2006.

[2] C. Arcoumanis and M. Gavaises. Linking nozzle flow with spray characteristics in a diesel fuel injection system. *Atomization and Sprays*, 8:307–347, 1998.

[3] C. Baumgarten. *Modellierung des Kavitationseinflusses auf den primären Strahlzerfall bei der Hochdruck-Dieseleinspritzung*. PhD thesis, University Hannover, 2003.

[4] C.E. Brennen. *Cavitation and Bubble Dynamics*. ISBN 0-19-509409. Oxford University Press, 1995.

[5] R. Busch. *Untersuchung von Kavitationsphänomenen in Dieseleinspritzdüsen*. PhD thesis, University Hannover, 2001.

[6] H. Chaves, M. Knapp, A. Kubitzek, F. Obermeier, and T. Schneider. Experimental study of cavitation in the nozzle hole of diesel injectors using transparent nozzles. *SAE*, (SAE 950290), 1995.

[7] N. Chigier and R.D. Reitz. Regimes of jet breakup and breakup mechanisms (physical aspects). *Recent Advances in Spray Combustion: Spray Atomization and Drop Burning Phenomena*, 1, 1996.

[8] S. Kampmann, B. Dittus, P. Mattes, and M. Kirner. The influence of hydro grinding at vco nozzles on the mixture preparation in a di diesel engine. *SAE*, (SAE 960867), 1996.

[9] E. Kull. *Einfluss der Geometrie des Spritzlochs von Dieseleinspritzdüsen auf das Einspritzverhalten*. PhD thesis, Universität Erlangen-Nürnberg, 2003.

[10] A. Nishimura and D.N. Assanis. A model for primary diesel fuel atomization based on cavitation bubble collapse energy. *Institute for Liquid Atomization and Spray Systems*, 2000.

[11] P. Pelloni and G.M. Bianchi. A cavitation-induced atomization model for high-preesure diesel spray simulations. *32 ISATA International Congress*, (99SIO44), 1999.

[12] R.D. Reitz. Modelling atomization processes in high-pressure vaporizing sprays. *Atomization and Spray Technology*, 3:309–337, 1987.

[13] R.D. Reitz and F.V. Bracco. Mechanisms of atomization of a liquid jet. *Phys. Fluids*, 1982.

[14] R.D. Reitz and F.V. Bracco. Mechanisms of breakup of round liquid jets. *Encyclopedia of Fluid Mechanics*, 3:233–249, 1986.

[15] R.D. Reitz and R. Diwakar. Structure of high-pressure fuel sprays. *SAE*, (SAE 870598), 1987.

[16] B.M. Schneider. *Experimentelle Untersuchungen zur Spraystruktur in transienten, verdampfenden und nicht verdampfenden Brennstroffstrahlen unter Hochdruck*. PhD thesis, Eidgenössischen Technischen Hochschule Zürich, 2003.

[17] M. Sommerfeld. *Modellierung und numerische Berechnung von Partikelbeladenen Strömungen mit Hilfe des Euler/Lagrange-Verfahrens*. Shaker Verlag, Aachen, 1996.

[18] J.O. Soriano Palao, M. Sommerfeld, A. Burkhardt, and H. Chaves. Modeling the influence of the nozzle flow on diesel spray atomization under high pressure injection conditions. *Institute for Liquid Atomization and Spray Systems*, 2007.

[19] C. Soteriou, R. Andrews, and M. Smith. Direct injection diesel sprays and the effect of cavitation and hydraulic flip on atomization. *SAE*, (950080), 1995.

[20] R. Tatschl, C. von Kuensberg Sarre, A. Alajbegovic, and E. Winklhofer. Diesel spray breakup modelling including multidimensional cavitating nozzle effects. *Institute for Liquid Atomization and Spray Systems*, 2000.

[21] E. von Berg, A. Alajbegovic, D. Greif, A. Poredos, R. Tatschl, E. Winklhofer, and L.C. Ganippa. Primary break-up model for diesel jets based on locally resolved flow field in the injection hole. *Institute for Liquid Atomization and Spray Systems*, 2002.

[22] E. von Berg, W. Edelbauer, A. Alajbegovic, R. Tatschl, M. Volmajer, B. Kegl, and L.C. Ganippa. Coupled simulations of nozzle flow, primary fuel jet breakup, and spray formation. *Journal of Engineering for Gas Turbines and Power*, Vol 127:897, 2005.

[23] P.J. Zwart, A.G. Gerber, and T. Belamri. A two-phase flow model for predicting cavitation dynamics. *International Conference on Multiphase Flow*, (Paper No 152), 2004.